

## PAIN

## Pharmacokinetics of ketamine and its major metabolites norketamine, hydroxynorketamine, and dehydronorketamine: a model-based analysis

Jasper Kamp\*, Kelly Jonkman, Monique van Velzen, Leon Aarts, Marieke Niesters, Albert Dahan and Erik Olofsen

Department of Anesthesiology, Leiden University Medical Center, Leiden, the Netherlands

\*Corresponding author. E-mail: [j.kamp@lumc.nl](mailto:j.kamp@lumc.nl)

### Abstract

**Background:** Recent studies show activity of ketamine metabolites, such as hydroxynorketamine, in producing rapid relief of depression-related symptoms and analgesia. To improve our understanding of the pharmacokinetics of ketamine and metabolites norketamine, dehydronorketamine, and hydroxynorketamine, we developed a population pharmacokinetic model of ketamine and metabolites after i.v. administration of racemic ketamine and the S-isomer (esketamine). Pharmacokinetic data were derived from an RCT on the efficacy of sodium nitroprusside (SNP) in reducing the psychotomimetic side-effects of ketamine in human volunteers.

**Methods:** Three increasing i.v. doses of esketamine and racemic ketamine were administered to 20 healthy volunteers, and arterial plasma samples were obtained for measurement of ketamine and metabolites. Subjects were randomised to receive esketamine/SNP, esketamine/placebo, racemic ketamine/SNP, and racemic ketamine/placebo on four separate occasions. The time–plasma concentration data of ketamine and metabolites were analysed using a population compartmental model approach.

**Results:** The pharmacokinetics of ketamine and metabolites were adequately described by a seven-compartment model with two ketamine, norketamine, and hydroxynorketamine compartments and one dehydronorketamine compartment with metabolic compartments in-between ketamine and norketamine, and norketamine and dehydronorketamine main compartments. Significant differences were found between S- and R-ketamine enantiomer pharmacokinetics, with up to 50% lower clearances for the R-enantiomers, irrespective of formulation. Whilst SNP had a significant effect on ketamine clearances, simulations showed only minor effects of SNP on total ketamine pharmacokinetics.

**Conclusions:** The model is of adequate quality for use in future pharmacokinetic and pharmacodynamic studies into the efficacy and side-effects of ketamine and metabolites.

**Clinical trial registration:** Dutch Cochrane Center 5359.

**Keywords:** ketamine; modelling; NONMEM; population pharmacokinetics; racemic ketamine; S-ketamine

**Editor's key points**

- Recent studies show that dehydronorketamine and hydroxynorketamine, the secondary metabolites of ketamine, may also possess analgesic and antidepressant effects.
- Little is known of the pharmacokinetics of these secondary metabolites.
- Non-linear mixed-effects modelling was used to study the pharmacokinetics of ketamine and its metabolites using data from a previous study of the effect of sodium nitroprusside on the psychotomimetic effects of ketamine and esketamine.
- The pharmacokinetics of ketamine, esketamine, norketamine, dehydronorketamine, and hydroxynorketamine were adequately described by a seven-compartment model.

Ketamine, first synthesised in the early 1960s, is currently experiencing a renewed interest with applications in a variety of indications. It was initially developed as dissociative anaesthetic and as a safer alternative to phencyclidine, causing less excitation upon emergence from anaesthesia.<sup>1</sup> Presently, ketamine is increasingly used for the treatment of acute (perioperative) pain, chronic neuropathic pain, and therapy-resistant clinical depression.<sup>1,2</sup> Whilst ketamine interacts with multiple receptor systems, its blockade of the N-methyl-D-aspartate receptor (NMDAR) is considered pivotal in producing anaesthesia, pain relief, and antidepressant effects.<sup>1,3</sup> Ketamine is a racemic mixture (RS-ketamine) and is available in two commercial formulations. The racemic mixture (Ketalar™; Pfizer, Berlin, Germany) has been available for many years and is used in human and veterinary medicine. More recently (since 1997), the S-enantiomer (Ketanest®; Eurocept Pharmaceuticals BV, Ankeveen, the Netherlands) has been marketed in various European countries for the same indications as RS-ketamine, whilst in 2019 esketamine for intranasal administration (Spravato™, Janssen-Cilag International, Belgium) was registered in the USA and the European Union for treatment of therapy-resistant depression.<sup>1,4,5</sup> There are substantial differences in potency between the S- and R-ketamine isomers. For example, S-ketamine has a two-fold greater anaesthetic potency relative to the racemic,<sup>6</sup> whereas the antidepressant effects of R-variant are three times more potent than those of S-ketamine.<sup>1</sup>

Ketamine is extensively metabolised by cytochrome P450 enzymes, particularly by CYP2B6 and CYP3A4.<sup>5,7</sup> The main metabolic pathway involves demethylation to norketamine, which is subsequently metabolised to dehydronorketamine (DHNK) and hydroxynorketamine (HNK).<sup>1,8</sup> These secondary metabolites, DHNK and HNK, were for a long time considered inactive or clinically irrelevant. However, recent studies showed activity of HNK in producing analgesia and antidepressant effects.<sup>1,9,10</sup> Little is known about the pharmacokinetic behaviour of these metabolites in humans. We found just one study, performed in nine patients with bipolar depression, which included DHNK and HNK in a pharmacokinetic analysis.<sup>11</sup> In the current study, we performed a population pharmacokinetic modelling study of ketamine and its metabolites (norketamine, DHNK, and HNK) after administration of escalating

doses of the racemic mixture and S-ketamine in 20 healthy volunteers. In this study, both drugs were administered without and with a continuous infusion of the nitric oxide donor sodium nitroprusside (SNP). Sodium nitroprusside was used to assess its ability to attenuate the schizotypal side-effects of ketamine. The descriptive results of this study have already been published.<sup>12</sup> The main aim of this secondary analysis was to develop a mixed-effects population pharmacokinetic model for ketamine and its most important metabolites.

**Methods****Ethics and subjects**

The current study is part of a large project on the efficacy of SNP in reducing the central and peripheral adverse effects of RS- and S-ketamine (e.g. drug high, schizotypal symptoms, and increased cardiac output). Secondary analyses were planned: (i) development of a population pharmacokinetic model of RS- and S-ketamine and their metabolites, (ii) pharmacokinetic–pharmacodynamic modelling of the analgesic and psychotomimetic effects of RS- and S-ketamine ketamine, and (iii) pharmacokinetic–pharmacodynamic modelling of the effects of RS- and S-ketamine on cardiac output. Here, we report on Item (i). The study protocol was approved by the Institutional Review Board of Leiden University Medical Centre (Commissie Medische Ethiek, Leiden, the Netherlands) and the Central Committee on Research Involving Human Subjects (Centrale Commissie Mensbonden Onderzoek, The Hague, the Netherlands). The study was registered at the trial register of the Dutch Cochrane Center ([www.trialregister.nl](http://www.trialregister.nl)) under identifier 5359. All procedures were performed in compliance with the latest version of the Declaration of Helsinki and Good Clinical Practice guidelines.

Subject enrolment was performed as previously published.<sup>12</sup> In brief, healthy male subjects, aged 18–34 yr and with a maximum BMI of 30 kg m<sup>-2</sup>, were recruited. For a complete list of exclusion criteria, see Jonkman and colleagues.<sup>12</sup> Importantly, subjects were excluded when they used any medication or herbs/vitamins in the 3 months before dosing. Additionally, they were not allowed to consume any caffeinated food or beverages in the 24 h before dosing, or consume any grapefruit-containing food or beverages in the 7 days before dosing. No consumption of any food or drinks were allowed for 8 h before dosing.

**Study design****Drugs**

The study had a double-blind, crossover, and randomised design. All subjects were studied on four occasions, which were identical in their design, except for the drug combinations that were administered. On visits A and B, participants received escalating doses of i.v. RS-ketamine (Ketalar); on visits C and D, they received escalating doses of S-ketamine (Ketanest-S). Additionally, subjects received i.v. placebo on visits A and C, and i.v. SNP (0.5 mg kg<sup>-1</sup> min<sup>-1</sup>) on visits B and D. (The sequence of visits was randomised.) Ketamine and SNP were infused via two distinct i.v. access lines placed on the ipsilateral hand and arm. RS-ketamine was administered according to the following infusion scheme: 0–60 min (0.28 mg kg<sup>-1</sup> h<sup>-1</sup>), 60–120 min (0.57 mg kg<sup>-1</sup> h<sup>-1</sup>), and 120–180 min (1.14 mg kg<sup>-1</sup> h<sup>-1</sup>). The equivalent S-ketamine infusion

scheme was 0–60 min (0.14 mg kg<sup>-1</sup> h<sup>-1</sup>), 60–120 min (0.28 mg kg<sup>-1</sup> h<sup>-1</sup>), and 120–180 min (0.57 mg kg<sup>-1</sup> h<sup>-1</sup>). The difference in dosing was based on observations that S-ketamine has twice the potency compared with RS-ketamine based on a pilot study, in which psychedelic symptoms were evaluated after a 50 mg dose of both drugs.

### Randomisation and blinding

The sequence of the study visits was randomised using a computer-generated randomisation list with a four-block design (www.randomization.org). The pharmacy was informed on the day before the study visit of the subject weight and subject and visit codes (visits A–D). The pharmacy prepared the medication on the morning of the study visit according to Good Manufacturing Practice guidelines and the randomisation list. Two syringes containing ketamine (RS-/S-ketamine) and placebo/SNP were dispensed to the research team in 50 ml syringes marked with the numerical subject and visit code and treatment (ketamine or SNP), ensuring full blinding of the research team. The research team remained blinded until all data were collected.

### Blood sampling and analysis

Arterial blood samples (8 ml) were obtained on each occasion at predefined sampling times:  $t=0$  (baseline), and 2, 6, 30, 59, 62, 66, 100, 119, 122, 126, 150, 179, 182, 186, 195, 210, and 300 min after the start of ketamine infusion. Samples were drawn from an arterial line, which was placed in the radial artery of the arm opposite to the arm where the i.v. line was placed for drug infusion.

Plasma samples were analysed in the laboratory of Dr Evan Kharasch (Washington University School of Medicine, St Louis, MO, USA) as extensively described by Rao and colleagues.<sup>13</sup> An enantioselective assay was used for ketamine, norketamine, and DHNK analyses. For HNK, total S- and R-concentrations were determined. For ketamine, norketamine, and DHNK, the lower and upper limits of quantitation were 2.5 and 250 ng ml<sup>-1</sup> and for HNK 5 and 500 ng ml<sup>-1</sup>.

## Population pharmacokinetic analysis

### Model development

To account for the differences in molecular weight between ketamine and the metabolites, concentration data were converted (from ng ml<sup>-1</sup> to nmol ml<sup>-1</sup>). Data analysis was performed in a stepwise fashion. First, the stereoselective ketamine data were analysed using a three-compartment model, similar to the published model by Sigtermans and colleagues.<sup>14</sup> Additionally, one- and two-compartment models were evaluated. Next, the best ketamine model was expanded by one to four metabolic delay compartments to model norketamine formation. As no norketamine was administered, the volume of the central norketamine compartment ( $V_1$ ) was not identifiable. It was therefore assumed that the volumes of the central ketamine and norketamine compartments were equal. As the kinetics of the central norketamine compartment could not be estimated from the data, we assumed that the amount of drug in the norketamine central compartment was in steady state (equilibrium) with respect to its peripheral and metabolism compartments.<sup>14</sup> Consequently, as the norketamine formation and elimination rates are then not both identifiable, the norketamine formation rate and ketamine

elimination rate were assumed equal.<sup>8,11,14</sup> Different norketamine models with one, two, or three norketamine compartments were fitted to the data. Finally, the optimal norketamine model was expanded with one to three metabolic compartments to model HNK and DHNK formation. Similar to norketamine, the volumes of DHNK and HNK  $V_1$  were not identifiable and therefore set equal to the volume of ketamine  $V_1$ , and the sum of the DHNK and HNK formation rates was set equal to the norketamine elimination rate. As no stereospecific HNK data were available, HNK formation was modelled as the sum from the separate S- and R-ketamine pathways.

To standardise the pharmacokinetic model parameters and to add body weight (WT) information to the model, clearances were allometrically scaled to litres per hour at 70 kg by  $CL=(WT/70)^{0.75}$ . Furthermore, compartment volumes were scaled to 70 kg body weight by  $V=WT/70$ . Model selection was based on a significant decrease in objective function value (OFV) calculated as  $-2 \log$  likelihood ( $\chi^2$  test, with  $P<0.01$  considered significant) and by assessing the goodness of fit by visual inspection of data fits and goodness-of-fit plots: normalised prediction distribution error vs time plots, normalised prediction distribution error vs predicted plots, and predicted vs measured plots. Moreover, prediction-variance-corrected visual prediction checks (VPCs) were performed by simulating 1000 data sets based on the model parameters and comparing the simulated quantiles with those of the true data.

### Statistical analysis

The data were analysed in NONMEM version 7.4.3 (ICON Development Solutions, Hanover, MD, USA). The M3 method for data censoring, as published by Beal,<sup>15</sup> was used for data below the level of quantitation and data above the upper limit of the calibration curve. LAPLACE-I estimation algorithm was used to estimate model parameters. To account for inter-individual and inter-occasion variability (IOV), random effects were included in the model with an exponential relation:  $\theta_i=\theta \times \exp(\eta_i+\eta_{ioV})$ , where  $\theta_i$  is the parameter for individual  $i$ ,  $\theta$  is the population parameter,  $\eta_i$  is the random difference between the population and individual parameter, and  $\eta_{ioV}$  is the difference between  $\theta_i$  and  $\theta$  as a result of IOV. In addition, proportional and additive errors were evaluated for each separate analyte to account for residual variability. The proportional and combined proportional and additive error models were described by  $Y_{ij}=F_{ij} \times (1+\epsilon_{ij})$  and  $Y_{ij}=F_{ij} \times (1+\epsilon_{1ij})+\epsilon_{2ij}$ , respectively, where  $Y_{ij}$  is the  $j$ th observed plasma concentration for individual  $i$ ,  $F_{ij}$  is the corresponding model prediction, and  $\epsilon_{ij}$  is the residual error. The standard error of the estimates (SEEs) was based on the covariance step of NONMEM without specifying a MATRIX option, so the default was used (i.e. the 'sandwich' matrix).

To test the effects of potential covariates, we performed a covariate search using an automated stepwise covariate screening algorithm (stepwise covariate model building module from PsN).<sup>16</sup> Characteristics included in the covariate testing were (i) analyte enantiomer (S- or R-isomer), (ii) placebo or SNP administration, and (iii) S-ketamine or RS-ketamine infused. Covariates were first tested by a forward search algorithm that sequentially added covariates that caused a significant reduction in OFV ( $P<0.01$ ) to the model. The relation between a covariate and a pharmacokinetic parameter was modelled as a linear relation with the following formula:  $\theta_i=\theta_{ref} \times (1+\theta_{COV})$ , where  $\theta_{ref}$  is the typical parameter value for a subject with the reference category of the covariate,

and  $\theta_{\text{COV}}$  is the effect of belonging to the non-reference category. The covariate causing the largest decrease in OFV was included in the first step of the forward search, followed by the covariate causing the second largest decrease. This process continued until either no covariates were left for inclusion or when the remaining covariates were unable to cause a significant decrease in OFV. The final forward model was used for the backward selection, in which a similar strategy was used, although now covariates were removed from the model. Removed covariates that did not cause a significant worsening of the OFV ( $P < 0.001$ ) were permanently excluded from the model. Covariates were maintained in the model when their removal caused a significant worsening of the OFV. This process continued until all covariates were excluded or until the covariates remaining in the model caused a significant worsening in OFV when removed.

### Simulations

The clinical relevance of the covariates that were added to the model by stepwise covariate model building was evaluated by simulation studies. The ketamine, norketamine, DHNK, and HNK concentration time relationships of escalating doses of ketamine infusions were simulated for a 70 kg individual and were performed using the RxODE package (version 0.8.0–9) for R studio (version 1.1.456; RStudio, Inc. Boston, USA). Three different conditions were simulated: S-ketamine after S-ketamine infusion, S-ketamine after RS-ketamine infusion, and R-ketamine after RS-ketamine infusion. Furthermore, the effect size of SNP was evaluated by simulating each of these conditions without and with infusions of SNP. To evaluate ketamine and metabolite concentrations in a clinical scenario, plasma concentrations were simulated for a typical 70 kg individual, after a dose of  $0.5 \text{ mg kg}^{-1}$  S-ketamine or RS-ketamine infused in 40 min.

## Results

All 20 subjects completed the four visits without serious adverse events. Mean (standard deviation) (range) subject body weight was 83 (9) (60–98) kg, height 186 (6) (175–193) cm, age 23 (2) (19–28) yr, and BMI 24.0 (2.1) (19.5–28.4)  $\text{kg m}^{-2}$ . Complete concentration curves were obtained in all subjects, with the exception for one visit of one subject as a result of inability to place the arterial line. A complete overview of the subject selection is shown in the Consolidated Standards of Reporting Trials flow chart (Supplementary Fig 1). Ketamine, norketamine, DHNK, and HNK concentrations are shown in Fig 1.

### Peak concentrations

An overview of peak concentrations ( $C_{\text{MAX}}$ ) with their respective times ( $T_{\text{MAX}}$ ) is shown in Supplementary Table 1. After racemic ketamine infusion, higher peak R-than S-enantiomer plasma concentrations were observed for ketamine, norketamine, and DHNK. Importantly, the concentration difference between the enantiomers increased with each metabolic step (i.e. the enantiomer concentration difference was greater for DHNK than for norketamine). Metabolite peak concentrations were delayed relative to the ketamine peak concentrations (ketamine  $T_{\text{MAX}}=170\text{--}173$  min) by 17 min for norketamine (irrespective of formulation) and 80–120 min for DHNK; the delay in HNK peak concentration was 81 min after S-ketamine

infusion and 69–72 min after racemic ketamine. Note, however, that not all subjects reached their HNK and DHNK  $C_{\text{MAX}}$  within the sampling time (Fig 1). For ketamine, 12% of measured plasma concentrations ( $n=241$ ) were below or above the lower and upper levels of quantitation, for norketamine 6.6% ( $n=127$ ), for DHNK 30% ( $n=580$ ), and for HNK 14% ( $n=149$ ).

### Structural pharmacokinetic model

The final model structure is shown in Fig 2. Ketamine pharmacokinetics were best described by a two-compartment model (OFV=–6976). Adding significant covariates resulted in a further improvement of the ketamine model to an OFV of –7130 points (Table 1). Norketamine was best modelled with two norketamine disposition compartments (OFV=–8635). Extending the model by adding two metabolic delay compartments for the norketamine formation improved the model by 70 points. The model was further improved by 702 points after addition of covariates. It was not possible to estimate the separate norketamine fractions that were metabolised to DHNK and HNK. We considered three different conditions with different fixed fractions for the DHNK and HNK formation 30%:70%, 40%:60%, and 50%:50% (DHNK%:HNK%) from norketamine to overcome structural parameter un-identifiability. Based on the observed plasma concentrations (Fig 1; Supplementary Table 1), we assumed that the fraction 30%:70% was most realistic and present the data analysis using this conversion rate. Dehydronorketamine was best modelled with one metabolic delay compartment and one disposition compartment (OFV=–9212). The covariates caused a further OFV reduction of 2349 points. In contrast, one HNK metabolic compartment coupled to one HNK disposition compartment showed a clear discrepancy in the elimination phase in the VPC. A model with two disposition compartments without a metabolic compartment solved this problem (OFV=–5106). Adding covariates further improved the model by 26 points.

### Pharmacokinetic model parameters

To get an indication of the best, median, and worst fits based on the coefficient of determination ( $R^2$ ), model fits are given in Fig 3 for pooled ketamine (Fig. 3a–c), norketamine (Fig. 3d–f), DHNK (Fig. 3g–i), and HNK (Fig. 3j–l) data sets. Goodness-of-fit plots are given in Supplementary Fig 2, showing a small misfit for R- and S-ketamine (Supplementary Fig 2a and b); the model slightly overestimates ketamine plasma concentrations at the lower concentration ranges. Otherwise, data fits and goodness-of-fit plots indicate that the model adequately describes the data. Visual predictive checks are given in Supplementary Figs 3–6. No overt misfits became apparent with 95% of measured data points within the 95% prediction intervals for the simulated ketamine, norketamine, and HNK data; for DHNK, some of the data points at the highest dose (180 min) lie above the 95% prediction interval. The simulated 95% prediction intervals of the proportions of the data under the lower limit of quantitation (LLOQ) or above the upper limit of quantitation were generally in agreement with the observed proportions. For HNK, a small misfit was observed for the proportion of the data under the LLOQ at the beginning of the sampling scheme (Supplementary Fig 6b). The observed proportion of 0.5 was attributable to the limited number of samples, in which HNK could be detected ( $n=2$ ). Of these two

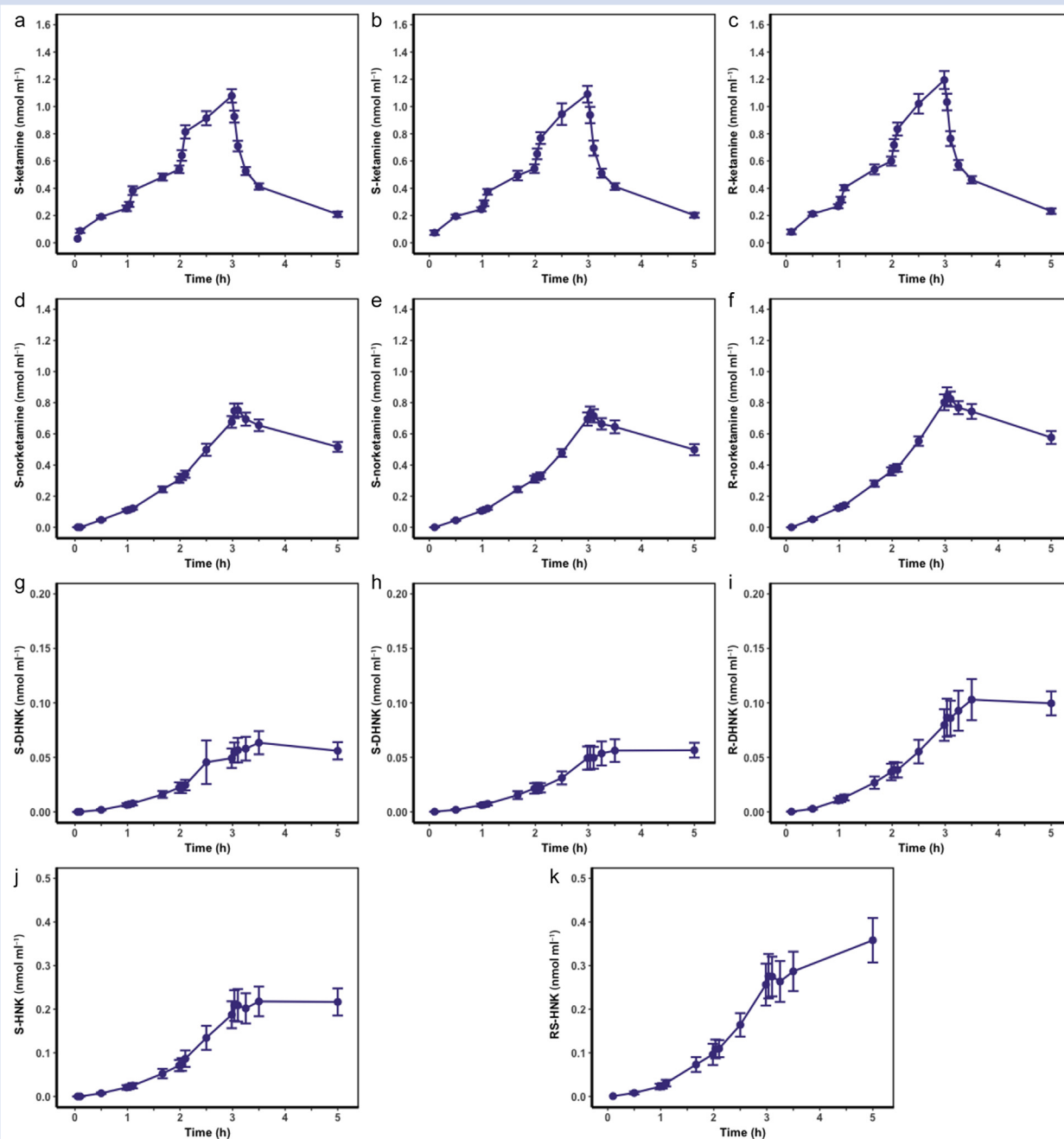
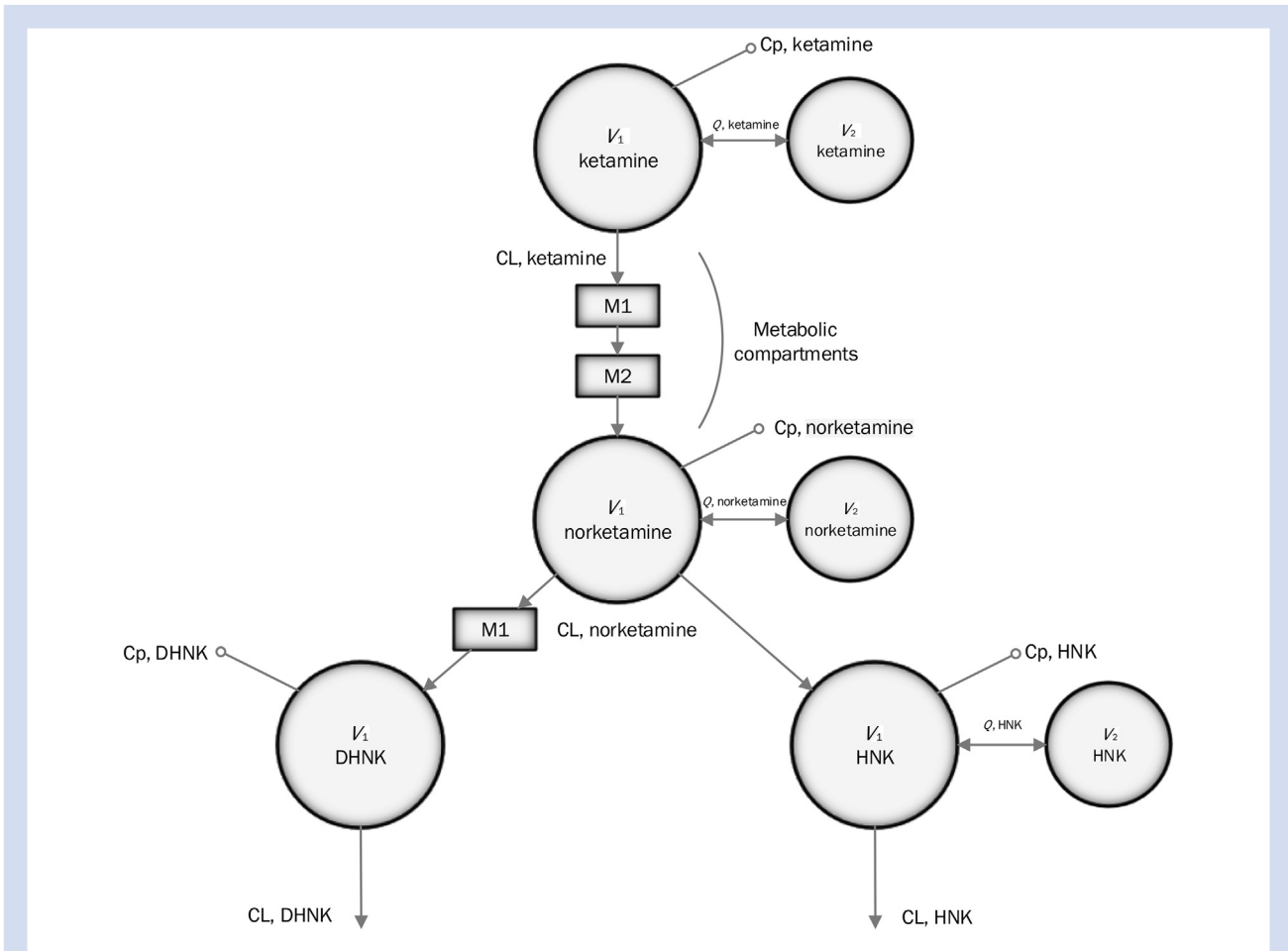


Fig. 1. Mean plasma concentrations (standard error) of (a, d, and g) S-ketamine, S-norketamine, and (b, e, and h) S-DHNK after esketamine; (c, f, and i) S-ketamine, S-norketamine, and S-DHNK after racemic; R-ketamine, R-norketamine, and R-DHNK after racemic ketamine administration; and (j) total HNK plasma concentrations after racemic ketamine. DHNK, dehydronorketamine; HNK, hydroxynorketamine.

samples, one sample was above the LLOQ and one sample was under the LLOQ and could therefore not be reliably quantified.

Parameter estimates and included covariates are given in Table 1. The R-enantiomers of ketamine, norketamine, and DHNK had an 11.5–49.3% lower elimination clearance than their (S)-variants. For ketamine, concomitant administration of SNP was associated with 9.2% increase in elimination and

21.6% increase in inter-compartmental clearance. As HNK plasma concentrations were not measured stereoselectively, only the effects of the formulation (racemic and S-ketamine) and concomitant infusion of SNP or placebo could be tested. Sodium nitroprusside had no effect on HNK pharmacokinetics. After RS-ketamine infusion, the HNK inter-



**Fig. 2.** Schematic overview of the final pharmacokinetic model for ketamine, norketamine, DHNK, and HNK.  $V_1$ , ketamine;  $V_2$ , ketamine;  $CL$ , ketamine; and  $Q$ , ketamine represent the central and peripheral ketamine compartments and the ketamine elimination and inter-compartmental clearances, respectively. Norketamine formation is modelled via two metabolic compartments (M1–2).  $V_1$ , norketamine;  $V_2$ , norketamine;  $CL$ , norketamine; and  $Q$ , norketamine represent the central and peripheral norketamine compartments and norketamine elimination and inter-compartmental clearances, respectively. DHNK formation from norketamine was modelled via one metabolic compartment (M1). DHNK was modelled with one disposition compartment ( $V_1$ , DHNK) with elimination clearance  $CL$ , DHNK. No metabolic compartments were used for the formation of HNK from norketamine.  $V_1$ , HNK and  $V_2$ , HNK represent the central and peripheral HNK compartments, respectively, with elimination clearance  $CL$ , HNK and inter-compartmental clearance  $Q$ , HNK.  $CL$ , elimination clearance; DHNK, dehydronorketamine; HNK, hydroxynorketamine;  $Q$ , inter-compartmental clearance.

compartmental clearance increased by 114% relative to just S-ketamine infusion.

### Simulations

In addition to the automated covariate search, the exploration of the importance of the included covariates was assessed through simulations. The effect of the two formulations (racemic vs S-ketamine) and co-administration of SNP or placebo on plasma concentrations was simulated using the same infusion paradigm as in the experimental study (Fig 4). Overall, the effects of the covariates were small. The administration of SNP caused small (<10%) reductions in peak S- and R-ketamine concentrations, irrespective of the formulation (red vs blue [placebo] lines in Fig. 4a–c), which is explained by the higher

ketamine clearances during SNP administration. However, this difference was not seen for the metabolites. The formulation had no effect on the S-ketamine plasma concentrations. The peak R-ketamine concentration after racemic ketamine infusion was higher than the S-ketamine concentrations after racemic or S-ketamine infusion. This effect was about 10%, which is attributable to the lower R-than S-ketamine clearance. Similarly, the peak R-norketamine and R-DHNK concentrations were higher than the S-variant after racemic ketamine infusion by factors 1.2 and 1.7, respectively. Although no stereoselective data were obtained for HNK, the simulations (that considered S-HNK formation after S-ketamine infusion; Fig 4j) suggest that after racemic ketamine infusion, the R-enantiomer was produced slower with a lower peak concentration than the S-variant (Fig 4k and l). The

**Table 1** Population pharmacokinetic model parameters. Central compartment volumes ( $V_1$ ) for norketamine, DHNK, and HNK were assumed to be equal to that of ketamine. CL, elimination clearance; DHNK, dehydronorketamine; HNK, hydroxynorketamine; MTT, mean transition time; Q, inter-compartmental clearance; SEE, standard error of the estimate; SNP, sodium nitroprusside;  $V_1$ , volume central compartment;  $V_2$ , volume peripheral compartment; %CV, % coefficient of variation, calculated as the SEE/typical parameter value\*100

	Parameter estimates		
	Typical parameter value (SEE) (%CV)	Inter-individual variability (%) (SEE) (%CV)	Inter-occasion variability (SEE) (%CV)
<b>Ketamine</b>			
$V_1$ (L [70 kg] <sup>-1</sup> )	25.8 (1.5) (6)	20.2 (4.85) (24)	20 (2.60%) (13)
$V_2$ (L [70 kg] <sup>-1</sup> )	115 (5.8) (5)	17.6 (2.82) (16)	—
CL (L h <sup>-1</sup> at 70 kg)	106.8 (3.2) (3)	10.7 (1.5) (14)	10.3 (0.93%) (9)
Q (L h <sup>-1</sup> at 70 kg)	126 (6.3) (5)	20.5 (5.13) (25)	—
Additive error (nmol L <sup>-1</sup> )	38.9 (2.3) (6)	—	—
Proportional error	0.108 (0.006) (6)	—	—
<b>Covariates</b>			
CL (% decrease when R-ketamine)	11.5 (0.58) (5)	—	—
CL (% increase when SNP)	9.2 (2.22) (24)	—	—
Q (% increase when SNP)	21.6 (5.18) (24)	—	—
<b>Norketamine</b>			
$V_2$ (L [70 kg] <sup>-1</sup> )	240 (19.2) (8)	25.2 (4.28) (17)	36 (3.24%) (9)
CL (L h <sup>-1</sup> at 70 kg)	59.9 (3.6) (6)	—	—
Q (L h <sup>-1</sup> at 70 kg)	196.2 (9.8) (5)	19.7 (3.35) (17)	24.2 (2.42%) (10)
MTT (min)	26.6 (2.1) (3)	—	—
Additive error (nmol L <sup>-1</sup> )	—	—	—
Proportional error	0.12 (0.005) (4)	—	—
<b>Covariates</b>			
CL (% decrease when R-norketamine)	26.9 (2.15) (8)	—	—
Q (% decrease when R-norketamine)	22.1 (2.43) (11)	—	—
<b>Dehydronorketamine</b>			
CL (L h <sup>-1</sup> at 70 kg)	185.4 (20.39) (11)	44.1 (7.5) (17)	21.2 (2.12%) (10)
MTT (min)	36.9 (2.95) (8)	36.9 (29.52) (8)	—
Additive error (nmol L <sup>-1</sup> )	1.82 (0.25) (14)	—	—
Proportional error	0.141 (0.01) (7)	—	—
<b>Covariates</b>			
CL (% decrease when R-DHDK)	49.3 (3.94) (8)	—	—
MTT (% increase when racemic ketamine)	20 (12.2) (61)	—	—
MTT (% decrease when R-DHDK)	16.1 (13.36) (83)	—	—
<b>Hydroxynorketamine</b>			
$V_2$ (L [70 kg] <sup>-1</sup> )	216 (41) (19)	—	—
CL (L h <sup>-1</sup> at 70 kg)	76.2 (20.60) (27)	86 (21.5) (25)	62.4 (7.49%) (12)
Q (L h <sup>-1</sup> at 70 kg)	218.4 (45.90) (21)	64.4 (23.18) (36)	34.6 (6.23%) (18)
Additive error (nmol L <sup>-1</sup> )	5.88 (1.2) (20)	—	—
Proportional error	0.249 (0.01) (8)	—	—
<b>Covariates</b>			
Q (% increase when racemic)	114 (39.9)	—	—

simulations for the clinical scenario (Fig 5) show plasma concentrations of norketamine (red line) and HNK (purple line) that eventually exceed ketamine concentrations.

## Discussion

In this study, the plasma concentrations of ketamine and three of its most important metabolites, norketamine, DHNK, and HNK, after escalating doses of racemic ketamine and esketamine, were quantified and analysed using a population pharmacokinetic model. Whilst often not considered clinically relevant, the importance of the metabolite HNK and to a lesser extent DHNK came to light in recent years, as these metabolites may be responsible for a (large) part of the antidepressant properties of ketamine.<sup>1-10</sup> Additionally, HNK has been shown

to produce analgesia in rodent pain models, without the schizotypal side-effects that obstruct the use of ketamine in chronic pain treatment.<sup>9</sup> An extensive understanding of the pharmacokinetics of ketamine and its metabolites is therefore of importance and will not only increase our knowledge of the pharmacokinetics of ketamine and its metabolites *per se*, but will also allow the design of precise infusion schemes for specific indications.

Ketamine is extensively metabolised in the liver.<sup>17</sup> The major metabolic pathway is through N-demethylation by hepatic enzymes CYP2B6 and CYP3A4 into norketamine.<sup>5-7</sup> Norketamine is subsequently metabolised to HNK by CYP2B6 and CYP2A6 enzymes or to DHNK by CYP2B6 (dehydrogenation). Furthermore, some DHNK may be produced from HNK through dehydration. Minor metabolic pathways that

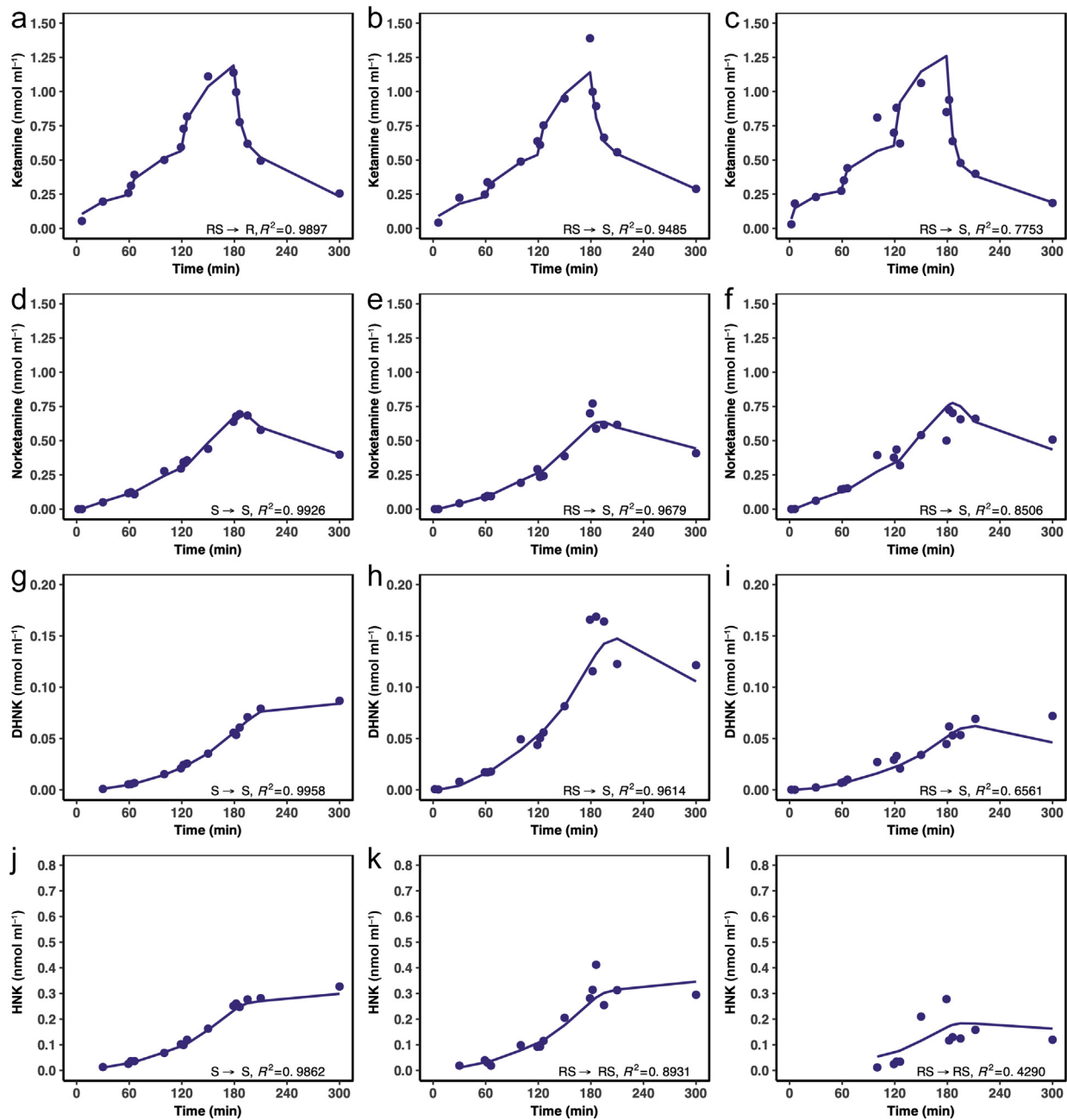


**Fig. 3.** Pharmacokinetic model fits. Best (left panels), median (centre panels), and worst (right panels) fits for (a–c) pooled ketamine, (d–f) norketamine, (g–i) DHNK, and (j–l) HNK data sets. The circles represent the true data. The lines are the model fits. DHNK, dehydronorketamine; HNK, hydroxynorketamine.

produce low-abundance metabolites include hydroxylation of ketamine to hydroxyketamine or hydroxyphenylketamine.<sup>10</sup> Given the relative unimportance of these minor pathways, we modelled the major metabolic ketamine pathway and assumed that DHNK and HNK are both produced from norketamine in a 30:70 ratio. The resultant pharmacokinetic model (Fig 2) was able to adequately describe the concentration-time data of the stereoisomers of ketamine, norketamine, and DHNK, and the sum of R- and S-HNK. Total HNK

was modelled as we were unsuccessful in measuring the individual HNK stereoisomers. Still, we were able to predict S- and R-HNK formation in our simulations (Fig 4k and l). We did not model DHNK formation from HNK as we assumed that just minute quantities of HNK were transformed into DHNK. Additionally, adding this metabolic pathway would have increased the complexity, and therefore decreased the stability of the model with consequently less reliable parameter estimates.



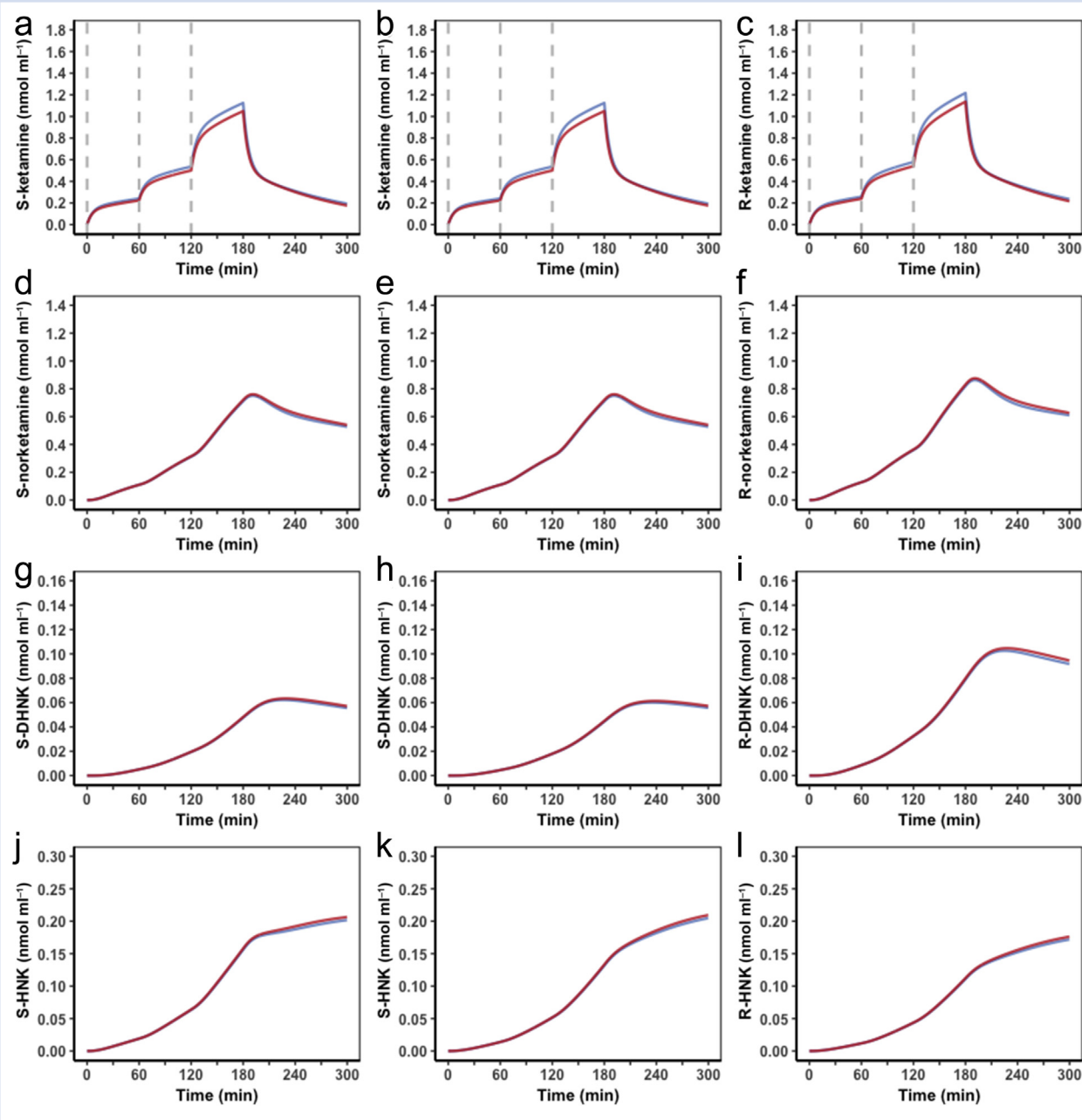
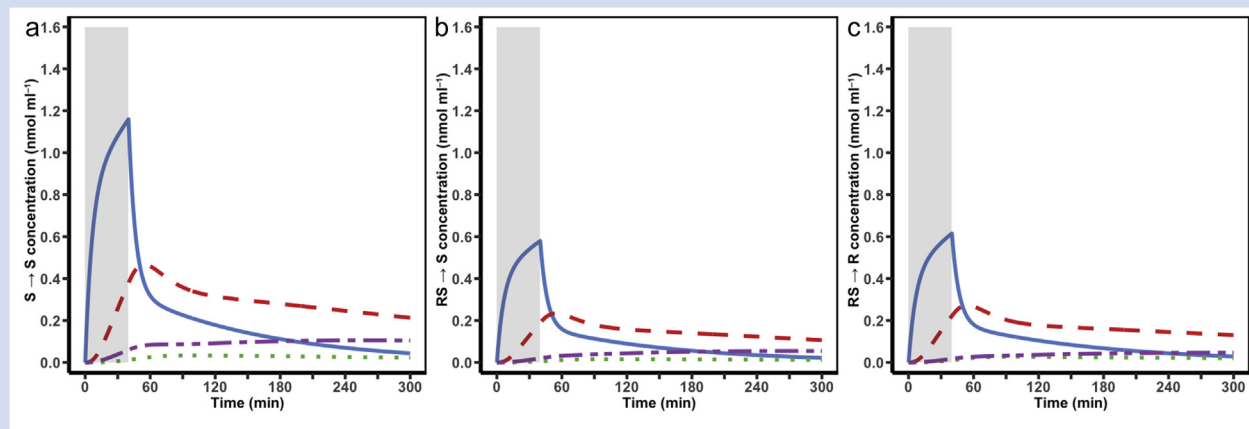


Fig. 4. Model simulations. Simulated concentration time profiles for a 70 kg individual after receiving escalating esketamine infusions (left panels) or racemic ketamine (centre and right panels) and with concomitant placebo administration (blue lines) or with SNP (red lines). Grey lines indicate the start of each ketamine dose. DHNK, dehydronorketamine; HNK, hydroxynorketamine.

Our analysis indicates major differences in S- and R-enantiomer pharmacokinetics, irrespective of their origin, with significant higher concentrations of R-ketamine, R-norketamine, and R-DHNK than the corresponding S-enantiomers (Fig 1). This corresponded with an up to 50% reduced elimination clearance of the R-compared with the S-enantiomers. It is generally accepted that S-enantiomer metabolism is favoured over R-enantiomer metabolism and is partly explained by the higher affinity of S-ketamine for the CYP3A4 enzyme.<sup>1,18–21</sup> Similar S- and R-enantiomer profiles were

reported by Zhao and colleagues.<sup>11</sup> They studied nine patients with treatment-resistant bipolar depression after daily treatment with  $0.5 \text{ mg kg}^{-1}$  racemic ketamine given over 40 min on 3 subsequent days. Zhao and colleagues analysed concentration–time data during the initial 230 min after RS-ketamine administration and on the subsequent 3 days post-infusion (in total, nine samples per subject were obtained), and constructed a population pharmacokinetic model that was made up of three ketamine, two norketamine, and single HNK and DHNK compartments (no metabolism



**Fig. 5.** Simulations in clinical context. Concentration time profiles of ketamine, norketamine, DHNK, and HNK (blue, red, green, and purple lines, respectively) after (a)  $0.5 \text{ mg kg}^{-1}$  esketamine or (b and c) racemic ketamine in a 70 kg individual. Note that, as racemic ketamine consists for 50% out of S-ketamine and for 50% out of R-ketamine, (b and c) peak concentrations for S-ketamine and R-ketamine after racemic ketamine are approximately half of the S-ketamine peak concentration after esketamine. Highlighted area indicates duration of infusion. DHNK, dehydronorketamine; HNK, hydroxynorketamine.

compartments were included). Similar to our data, they observed an S:R concentration ratio  $<1$  for ketamine and DHNK, whilst no enantioselectivity was observed for norketamine. Alike our analysis, only total HNK was measured in the study of Zhao and colleagues.<sup>11</sup> In contrast to our study, they observed that DHNK was the main metabolite in four of their subjects, norketamine in three subjects, and HNK in two subjects. In our study, total plasma HNK concentrations were approximately two times higher than the sum of S- and R-DHNK, which suggests that HNK formation is favoured over DHNK formation during the first 5 h after ketamine administration. Possibly, the higher DHNK production observed by Zhao and colleagues<sup>11</sup> was related to the longer sampling times.

A clinically important observation from the simulation study (Fig 5) is that after a similar ketamine dose of  $0.5 \text{ mg kg}^{-1}$  given over 40 min (the dose used in the treatment of therapy-resistant depression), racemic ketamine HNK plasma concentrations are higher than after S-ketamine administration (i.e. the sum of R- and S-HNK concentrations after racemic ketamine exceeds S-HNK concentrations after S-ketamine administration). This suggests that when higher HNK concentrations are needed to improve treatment efficacy, the racemic formulation is to be preferred over S-ketamine. Additionally, from the simulation, we infer lower R-than S-HNK concentrations, which we attribute to the slower formation of R-HNK. In rats, Moaddel and colleagues<sup>22</sup> show higher 2S,6S-HNK concentrations after S-ketamine infusion compared with 2R,6R-HNK after R-ketamine infusion. These data agree with our simulation data. However, a major limitation of our study is the restriction of HNK concentration data to 5 h after the start of ketamine infusion. As a consequence, we may have missed peak HNK data occurring at later times. Hence, we cannot draw definite conclusions regarding a possible difference in R- and S-HNK pharmacokinetics in our data set.

Previous studies suggested differences in S-ketamine pharmacokinetics after administration of S-ketamine vs racemic ketamine as a result of the inhibition of S-ketamine

metabolism by the R-enantiomer.<sup>20</sup> We were unable to detect significant differences in S-ketamine pharmacokinetics after either formulation. Hence, the clinical relevance of formulation (i.e. a formulation with or without R-ketamine) on S-ketamine pharmacokinetics therefore remains debatable.

In two arms of the study, we infused SNP. This was done to evaluate a possible modifying effect of SNP on the ketamine-induced schizotypal effects.<sup>12</sup> Additionally, SNP may reduce blood pressure elevations that coincide with ketamine treatment as a result of ketamine-induced sympatho-excitation.<sup>12</sup> Importantly, SNP will cause vasodilation that may lead to increased distribution of ketamine. The observed increases in terminal and inter-compartmental clearances were moderate (effect on ketamine CL and Q, 9% and 22%, respectively) and were restricted to ketamine. Based on the simulations (Fig 4), the effect of SNP on the complete pharmacokinetic picture seems limited. This further supports our hypothesis that the mitigating effect of SNP on psychotomimetic side-effects of racemic ketamine is not pharmacokinetically driven, but is related to the restoration of ketamine-induced depletion of intracellular nitric oxide, which restores neuroprotective effects from NMDAR activation.

The study has several limitations that warrant further commenting. First, the central volumes of distribution for all metabolites were set equal to the ketamine central volume of distribution. This was needed because of non-identifiability of these metabolite compartments. This might introduce bias to the estimation of metabolite clearances and peripheral compartment volumes. Administration of the metabolites or measurement of (glucuronide)-metabolites in urine could help solve this problem. However, norketamine, DHNK, and HNK are currently not available for human use. Second, we were unable to estimate the parent fraction converted into metabolites. In agreement with other studies, we assumed that ketamine was fully transformed into norketamine.<sup>8 11 14</sup> This assumption may have influenced the parameter estimates of the formation of secondary metabolites from norketamine. The assumption of a 30%:70% ratio (DHNK:HNK) is based on the measured plasma concentrations and was

needed to overcome structural parameter un-identifiability. Although modification of the formation ratio resulted in a change in DHNK and HNK clearances and HNK peripheral volume of distribution proportional to the different ratios used for DHNK and HNK formation, no effects on the objective function were observed. Third, the 5 h sampling time may have been sufficient for reliable estimation of ketamine and norketamine model parameters, but as indicated previously, this time profile may have been insufficient to properly characterise the pharmacokinetics of the secondary ketamine metabolites. Sampling up to 24–48 h post-dose would be likely to obtain sufficient data on secondary metabolite kinetics. Possibly, the estimate of the high DHNK elimination clearance was related to this issue. As no second compartment could be estimated for DHNK, no inter-compartmental clearance parameter was estimated. Conceivably, the elimination clearance may be the sum of a (non-identified) inter-compartmental clearance and the elimination clearance. Additionally, fixing the DHNK formation rate to 30% of the norketamine elimination rate may have overestimated the DHNK metabolic pathway.

In conclusion, we performed a population pharmacokinetic modelling study of ketamine and its major metabolites. Differences in pharmacokinetics between formulations and enantiomers were identified. Most importantly, we observed differences between S- and R-enantiomer elimination clearances. Another relevant observation was the absence of significant clinical effect of SNP on ketamine pharmacokinetics. This indicates that our previous finding that the attenuation by SNP of the psychotomimetic effects of racemic ketamine is not pharmacokinetically driven.<sup>12</sup> Despite some limitations, our model is likely to be of sufficient quality to be used in future pharmacokinetic and pharmacodynamic studies into the efficacy and side-effects of ketamine and its metabolites.

### Authors' contributions

Study conception: MN, AD  
 Project inception: LA, MN, AD, MvV  
 Project supervision: AD, MvV, LA  
 Writing of protocol: MN, AD, MvV  
 Experimentation: KJ, MN, AD  
 Experiment supervision: MvV, MN, AD  
 Data analysis: JK, EO  
 Writing of paper: JK, AD, EO  
 Reading of paper: KJ, MvV, LA, MN  
 Reviewing of paper: MvV, MN  
 Approval of paper: all authors

### Declarations of interest

The authors report no conflict of interest. At the time of submission, AD was chairman of the Institutional Review Board of Leiden University Medical Center, but was not involved in the review of this study.

### Funding

Institutional and departmental sources.

### Appendix A. Supplementary data

Supplementary data to this article can be found online at <https://doi.org/10.1016/j.bja.2020.06.067>.

### References

- Zanos P, Moaddel R, Morris PJ, et al. Ketamine and ketamine metabolite pharmacology: insights into therapeutic mechanisms. *Pharm Rev* 2018; **70**: 621–60
- Kamp J, Van Velzen M, Olofsen E, Boon M, Dahan A, Niesters M. Pharmacokinetic and pharmacodynamic considerations for NMDA-receptor antagonist ketamine in the treatment of chronic neuropathic pain: an update of the most recent literature. *Expert Opin Drug Metab Toxicol* 2019; **15**: 1033–41
- Mion G, Villevieille T. Ketamine pharmacology: an update (pharmacodynamics and molecular aspects, recent findings). *CNS Neurosci Ther* 2013; **19**: 370–80
- Kaufman MB. Pharmaceutical approval update. *Pharm Ther* 2019; **44**: 251–4
- Yanagihara Y, Kariya S, Ohtani M, et al. Involvement of CYP2B6 in N-demethylation of ketamine in human liver microsomes. *Drug Metab Dispos* 2001; **29**: 887–90
- Schuttler J, Stanski DR, White PF, et al. Pharmacodynamic modeling of the EEG effects of ketamine and its enantiomers in man. *J Pharmacokinet Biopharm* 1987; **15**: 241–53
- Hijazi Y, Bouliou R. Contribution of CYP3A4, CYP2B6, and CYP2C9 isoforms to N-demethylation of ketamine in human liver microsomes. *Drug Metab Dispos* 2002; **30**: 853–8
- Noppers I, Olofsen E, Niesters M, et al. Effect of rifampicin on S-ketamine and S-norketamine plasma concentrations in healthy volunteers after intravenous S-ketamine administration. *Anesthesiology* 2011; **114**: 1435–45
- Kroin JS, Das V, Moric M, Buvanendran A. Efficacy of the ketamine metabolite (2R,6R)-hydroxynorketamine in mice models of pain. *Reg Anesth Pain Med* 2019; **44**: 111–7
- Lumsden EW, Troppoli TA, Myers SJ, et al. Antidepressant-relevant concentrations of the ketamine metabolite (2R,6R)-hydroxynorketamine do not block NMDA receptor function. *Proc Natl Acad Sci U S A* 2019; **116**: 5160–9
- Zhao X, Venkata SL, Moaddel R, et al. Simultaneous population pharmacokinetic modelling of ketamine and three major metabolites in patients with treatment-resistant bipolar depression. *Br J Clin Pharmacol* 2012; **74**: 304–14
- Jonkman K, van der Schrier R, van Velzen M, et al. Differential role of nitric oxide in the psychedelic symptoms induced by racemic ketamine and esketamine in human volunteers. *Br J Anaesth* 2018; **120**: 1009–18
- Rao LK, Flaker AM, Friedel CC, Kharasch ED. Role of cytochrome P4502B6 polymorphisms in ketamine metabolism and clearance. *Anesthesiology* 2016; **125**: 1103–12
- Sigtermans M, Dahan A, Mooren R, et al. S(+)-ketamine effect on experimental pain and cardiac output: a population pharmacokinetic-pharmacodynamic modeling study in healthy volunteers. *Anesthesiology* 2009; **111**: 892–903
- Beal SL. Ways to fit a PK model with some data below the quantification limit. *J Pharmacokinet Pharmacodyn* 2001; **28**: 481–504
- Lindbom L, Pihlgren P, Jonsson EN. PsN-Toolkit—a collection of computer intensive statistical methods for non-linear mixed effect modeling using NONMEM. *Comput Methods Progr Biomed* 2005; **79**: 241–57
- Peltoniemi MA, Hagelberg NM, Olkkola KT, Saari TI. Ketamine: a review of clinical pharmacokinetics and pharmacodynamics in anesthesia and pain therapy. *Clin Pharmacokinet* 2016; **55**: 1059–77

18. Goldberg ME, Torjman MC, Schwartzman RJ, Mager DE, Wainer IW. Enantioselective pharmacokinetics of  $R$ - and  $S$ -ketamine after a 5-day infusion in patients with complex regional pain syndrome. *Chirality* 2011; **23**: 138–43
19. Geisslinger G, Hering W, Thomann P, Knoll R, Kamp HD, Brune K. Pharmacokinetics and pharmacodynamics of ketamine enantiomers in surgical patients using a stereoselective analytical method. *Br J Anaesth* 1993; **70**: 666–71
20. Ihmsen H, Geisslinger G, Schuttler J. Stereoselective pharmacokinetics of ketamine:  $R$ -ketamine inhibits the elimination of  $S$ (+)-ketamine. *Clin Pharmacol Ther* 2001; **70**: 431–8
21. Henthorn TK, Avram MJ, Dahan A, et al. Combined recirculatory-compartmental population pharmacokinetic modeling of arterial and venous plasma  $S$ (+) and  $R$ (-) ketamine concentrations. *Anesthesiology* 2018; **129**: 260–70
22. Moaddel R, Sanghvi M, Dossou KSS, et al. The distribution and clearance of (2S,6S)-hydroxynorketamine, an active ketamine metabolite, in Wistar rats. *Pharmacol Res Perspect* 2015; **3**: 1–10

Handling editor: Tony Absalom